Chapter 15 A Real-Time Algorithm for Computing the Tension Force in a Suspended Elastic Sagging Cable



Aravind Baskar, Mark Plecnik, Jonathan D. Hauenstein, and Charles W. Wampler

Abstract An algorithm is presented for computing the tension in an elastic cable subject to sagging under its own weight, a problem highly relevant in tethered systems such as cable-driven parallel robots. This requires solving the two coupled equations of the Irvine cable model, which give the endpoint position as a function of vertical and horizontal components of tension. Via a change of variables, we reformulate this system as a pair of uncoupled equations, which are shown to have a unique solution. We develop an efficient numerical procedure to solve one of these, after which closed-form formulas provide the solution of the second equation and ultimately the tension components.

Keywords Sagging cable · Tension · Irvine model

15.1 Introduction

We present a solution for determining the tension force in a suspended sagging cable and its associated profile at equilibrium, given the end-coordinates and the unstrained length of the cable. This problem is highly relevant in tethered systems such as cable-driven parallel robots (CDPRs), where real-time estimation of cable tension force and profile is essential for effective planning and control. Due to the non-algebraic nature of the cable sag equations, which are highly sensitive to minor variations in geometric and material parameters, significant numerical challenges persist. A recent study in the literature proposed a semi-analytical approximate solution for a special case, assuming in-extensible cable properties [7]. However, for the general elastic sagging cable system given by the Irvine model [3], the prevailing real-time approach appears to involve the development of neural network models [6]. In this work, we introduce an alternative near-closed-form solution flow that entails reformulating the sagging cable model through a change of variables, thereby reducing

A. Baskar (⋈) · M. Plecnik · J. D. Hauenstein · C. W. Wampler University of Notre Dame, Notre Dame, IN 46556, USA e-mail: abaskar@nd.edu

it to the solution of a single equation in one variable. We prove that this resulting non-algebraic equation always has a unique solution for valid geometric and material parameters. The solution can be efficiently obtained in real-time using the secant method with initial guesses derived based on real analysis. The implementation of this algorithm addresses the outstanding computational challenges associated with determining cable tension forces and estimating cable profiles in large CDPRs and other tether cable systems.

15.2 Mathematical Model

Consider the schematic of a cable in the vertical **XZ**-plane with **O** as the origin coinciding with one end of the suspended cable as shown in Fig. 15.1. We assume gravity to act downwards along z-direction. We neglect all lateral static forces on the cable. This makes it a planar approximation model in the vertical plane. The cable is modeled as an elastic element capable of deforming under tension and sagging under its own weight. Let μ , A, and E be the physical properties associated with the cable, namely, linear density, cross sectional area, and the Young's modulus of the cable material, respectively. Let E be the unstrained length of the cable and E0 be the end-coordinates of the cable. Let E1 be the horizontal and vertical components of the tension, respectively. The kineto-statics equations which relate the end-coordinates, namely, E2 and the respective tension components E3 are:

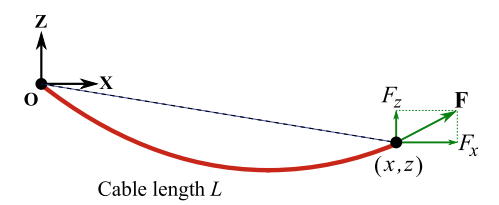
$$\begin{pmatrix} x \\ z \end{pmatrix} = \begin{pmatrix} F_x \left(\frac{L}{EA} + \frac{1}{\mu g} \left(\sinh^{-1} \left[\frac{F_z}{F_x} \right] - \sinh^{-1} \left[\frac{F_z - \mu g L}{F_x} \right] \right) \right) \\ \frac{F_z L}{EA} - \frac{\mu g L^2}{2EA} + \frac{1}{\mu g} \left(\sqrt{F_x^2 + F_z^2} - \sqrt{F_x^2 + (F_z - \mu g L)^2} \right) \end{pmatrix}.$$
 (15.1)

A necessary condition of the Irvine model for the cable to be in tension is

$$F_{\rm r} > 0. \tag{15.2}$$

In particular, Eq. (15.1) together with the inequality condition in Eq. (15.2) accounts for the configurations in the half-plane x > 0. Configurations in the half-plane where

Fig. 15.1 Irvine sagging cable model



x < 0 can be safely disregarded as they possess a mirror-symmetric equivalence relation.

Problem statement. Suppose that (x, z) and L are known. For example, (x, z) can be measured by an external measurement system such as a camera system and L can be measured via encoder data from cable pulleys or other position sensors. The objective is to determine the cable tension components (F_x, F_z) quickly and accurately so that they can be used in real-time to profile the cable. The challenge is that (F_x, F_z) are computed by solving the non-algebraic system of equations given by Eq. (15.1). For real-time computation, this is not straightforward due to the reliance on a good initial guess for (F_x, F_z) as well as the sensitivity of these forces to minor variations in the geometric and material parameters involved.

Recent work [1] developed an alternative, but mathematically equivalent cable model allowing cable sag, derived through a change of variables from (F_x, F_z) to (α, β) under the physically-meaningful assumptions that $\mu > 0$ and L > 0, namely:

The corresponding cable tension (F_x, F_z) in the vertical plane is then:

$$\begin{pmatrix} F_x \\ F_z \end{pmatrix} = \frac{\mu g L}{\sinh{[\alpha]} - \sinh{[\beta]}} \begin{pmatrix} 1 \\ \sinh{[\alpha]} \end{pmatrix}. \tag{15.4}$$

Equation (15.3) defines the sagging cable kineto-statics in terms of the new real variables (α, β) with a necessary operating condition that $\alpha > \beta$, which is equivalent to Eq. (15.2). Although Eq. (15.3) cannot be made algebraic as it contains both algebraic and exponential forms of α and β , it does define *Pfaff* manifolds [4]. Hence, one still obtains finiteness properties on the number of real roots for α, β given x, z, L. In particular, we show below that it admits a unique real root for all valid parameters.

To further simplify Eq. (15.3), the following linear change of variables is introduced:

$$\frac{1}{2}(\alpha + \beta) = \chi, \quad \frac{1}{2}(\alpha - \beta) = \psi.$$
 (15.5)

Hence, (α, β) can be expressed in terms of the new variables (χ, ψ) via:

$$\alpha = \chi + \psi, \quad \beta = \chi - \psi. \tag{15.6}$$

Moreover, the inequality condition $\alpha > \beta$ becomes $\psi > 0$.

Using the following identities:

$$\sinh [\chi + \psi] - \sinh [\chi - \psi] = 2 \cosh [\chi] \sinh [\psi],$$

$$\sinh [\chi + \psi] + \sinh [\chi - \psi] = 2 \sinh [\chi] \cosh [\psi],$$

$$\cosh [\chi + \psi] - \cosh [\chi - \psi] = 2 \sinh [\chi] \sinh [\psi],$$

Equation (15.3) can be rewritten as:

$$\begin{pmatrix} x \\ z \end{pmatrix} = \frac{L}{\sinh[\psi]} \begin{pmatrix} \left(\frac{\mu g L}{2EA} + \psi\right) \operatorname{sech}[\chi] \\ \left(\frac{\mu g L}{2EA} \cosh[\psi] + \sinh[\psi]\right) \tanh[\chi] \end{pmatrix},$$
 (15.7)

which is a representation of the Irvine cable model in terms of the variables (χ, ψ) . This model also presents a geometric understanding of the Irvine cable model. Here, $\psi > 0$ directly gives a measure of cable sag. The greater the value of ψ , the greater the cable sag for a given χ , with $\psi \to 0^+$ approaching a fully taut configuration. Moreover, the variable χ ranges from $-\infty$ to ∞ and roughly indicates the orientation of the cable axis within the cable half plane considered, x > 0. In this context, the term 'cable axis' refers to the line joining the cable endpoints. When $\chi = 0$, the cable axis is horizontal. Positive values of χ correspond to cable configurations in the quarter where z > 0, while negative values correspond to configurations in the quarter where z < 0. The limits at $\pm \infty$ represent vertical orientations of the cable

Using the following identity:

axis.

$$\operatorname{sech}^{2}[\chi] + \tanh^{2}[\chi] - 1 = 0,$$

Eq. (15.7) uncouples to become:

$$f(\psi) := \left(\frac{x_m \sinh [\psi]}{\varepsilon + \psi}\right)^2 + \left(\frac{z_m}{\varepsilon \coth [\psi] + 1}\right)^2 - 1 = 0, \quad (15.8)$$

$$\chi = \tanh^{-1} \left[\frac{z_m}{\varepsilon \coth \left[\psi \right] + 1} \right], \tag{15.9}$$

where $x_m = \frac{x}{L}$, $z_m = \frac{z}{L}$ and $\varepsilon = \frac{\mu gL}{2EA}$. Here, ε is a quantity equivalent to the strain of a vertical hung cable of length $\frac{L}{2}$ under its self-weight. More importantly, Eq. (15.8) is a univariate non-algebraic equation in ψ that can be solved for $\psi > 0$ using local methods and then Eq. (15.9) yields the corresponding value of χ from ψ . The following analyzes Eq. (15.8) to show that $f(\psi) = 0$ always has a unique solution with $\psi > 0$ for any given set of valid parameters.

15.3 Existence and Uniqueness

For $g(\psi) := \frac{\sinh[\psi]}{\varepsilon + \psi}$ and $h(\psi) := \frac{1}{\varepsilon \coth[\psi] + 1}$, the function $f(\psi)$ in Eq. (15.8) becomes

$$f(\psi) = x_m^2 g(\psi)^2 + z_m^2 h(\psi)^2 - 1 = 0,$$
 (15.10)

where the valid parameters correspond with real $x_m > 0$, z_m , and $\varepsilon > 0$. In order to show that $f(\psi)$ is *strictly increasing* for $\psi > 0$, it is sufficient to show that both $g(\psi)$ and $h(\psi)$ are positive-valued and strictly increasing themselves for $\psi > 0$.

- $-g(\psi)$: This function is positive for any $\psi > 0$ since $\sinh[\psi]$ is positive for $\psi > 0$. Furthermore, $g'(\psi) = \frac{\cosh[\psi]}{(\varepsilon + \psi)^2} (\varepsilon + \psi \tanh[\psi])$ is always greater than zero for $\psi > 0$. Thus, $g(\psi)$ is a positive-valued and strictly increasing function for $\psi > 0$.
- $-h(\psi)$: Since $\coth[\psi] > 0$ for $\psi > 0$, $h(\psi)$ is positive-valued. Additionally, the strictly decreasing nature of $\coth[\psi]$ for $\psi > 0$ proves that $h(\psi)$ is strictly increasing over the same domain.

Since $f(\psi)$ is strictly increasing for $\psi > 0$ with f(0) = -1 and $\lim_{\psi \to \infty} f(\psi) = \infty$, this shows that $f(\psi) = 0$ always has a unique root for $\psi > 0$.

With existence and uniqueness confirmed, the next step is to present a pathway to compute this root.

15.4 Initial Guess Function

In most metallic cable systems, $\varepsilon \to 0^+$ is a reasonable approximation in sagging configurations as E is large. This in-extensible cable approximation may be used to obtain a good initial guess to solve for ψ . In the limit of $\varepsilon \to 0^+$, $f(\psi) = 0$ becomes

$$x_m^2 \left(\frac{\sinh[\psi]}{\psi}\right)^2 + z_m^2 - 1 = 0.$$
 (15.11)

Since $\psi > 0$ and x > 0, Eq. (15.11) is equivalent to

$$\frac{\sinh{[\psi]}}{\psi} = k \text{ where } k = \frac{\sqrt{1 - z_m^2}}{x_m} = \frac{\sqrt{L^2 - z^2}}{x}.$$
 (15.12)

As expected, $\sinh [\psi]/\psi$ is strictly increasing for $\psi>0$ and limits to 1^+ as $\psi\to 0^+$. Hence, this approximation can only hold true when $x^2+z^2< L^2$ yielding k>1. As $k\to\infty$, it denotes configurations along the vertical axis, where $x\to 0$. It must be noted that in high tension taut configurations, the variable k may marginally drop below 1. Therefore, we will address both cases: k>1 and $k\le 1$ to obtain initial guesses for both scenarios.

15.4.1 k > 1

For the case of k > 1, we proceed by developing an implicit fixed-point rule based on Eq. (15.12), which is equivalent to:

$$\psi = \sinh^{-1} [k \ \psi]. \tag{15.13}$$

For deriving an explicit guess function ψ_0 , the fixed-point rule can be used in recursion with a starting basis function of the form $a(k-1)^b$ for 3 iterations:

$$\psi_0 = \sinh^{-1} \left[k \sinh^{-1} \left[k \sinh^{-1} \left[k a(k-1)^b \right] \right] \right].$$
 (15.14)

For a>0 and b>0, the starting basis function $a(k-1)^b$ is chosen based on the observation that in Eq. (15.13) we have $\psi\to 0^+$ when $k\to 1^+$ and ψ is strictly increasing with respect to k. The parameters (a,b) can be computed by performing a weighted numerical optimization to minimize error over $1< k<\infty$ in Eq. (15.13) via:

$$\operatorname{argmin}_{a>0,b>0} \int_{k=1}^{\infty} \left(\frac{\psi_0 - \sinh^{-1} \left[k \ \psi_0 \right]}{k} \right)^2 dk$$

yielding approximately a=2.120 and b=0.413. Figure 15.2 compares the proposed explicit function ψ_0 given by Eq. (15.14) against ψ defined implicitly by solving Eq. (15.13) which shows a good match.

As an alternative, a starting basis function of the form $a \cosh^{-1}[k]$ may also be considered, based on the analysis presented in [7][§ IV]. For this basis function, $a \cosh^{-1}[k]$, in conjunction with 3 fixed-point iterations, the optimal value of a is found to be 1.666.

The value ψ_0 given by Eq. (15.14) may already be accurate enough for many applications, but to obtain an even more accurate solution, one can use it as the initial

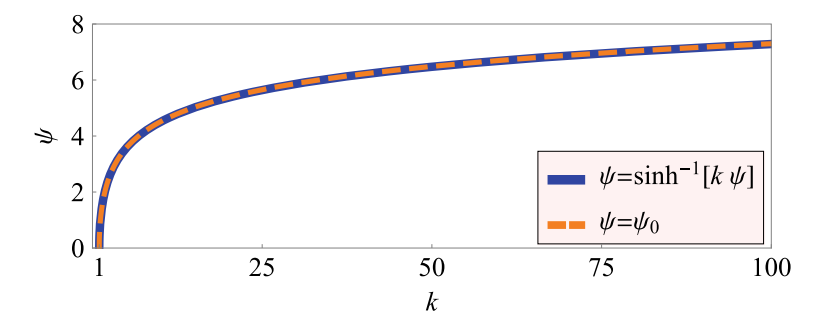


Fig. 15.2 Comparison of the proposed explicit guess function ψ_0 against the implicitly defined value satisfying the in-extensible cable model $\psi = \sinh^{-1}{[k \; \psi]}$

guess for a local root-finding method. To avoid computing the derivative required for Newton's method, we use the secant method instead. This requires a second guess, ψ_1 , which we obtain by solving a first order Taylor series approximation of Eq. (15.12) about ψ_0 :

$$\psi_1 = \psi_0 \left(1 + \frac{k\psi_0 - \sinh[\psi_0]}{\cosh[\psi_0] \psi_0 - \sinh[\psi_0]} \right).$$
(15.15)

Although the secant method has a lower convergence rate per iteration than Newton's method, its lower cost per iteration makes it the more efficient method.

15.4.2 $0 < k \le 1$

In the alternative case of $0 < k \le 1$, it happens that $\psi \to 0^+$, so ε dominates ψ . By Eq. (15.12), $x^2 + z^2 \ge L^2$, which means that the cable is in high tension, because even with zero weight it would be stretched beyond its natural length. For this case, by solving a second order approximation of $f(\psi)$ given by Eq. (15.8) about $\psi = 0$, we obtain the alternative guess pair $\psi_0 = 0$ and $\psi_1 = \frac{\varepsilon}{\sqrt{x_m^2 + z_m^2}}$. As before, the guesses, ψ_0, ψ_1 , are used to initialize the secant method to solve for ψ .

15.5 Numerical Algorithm

Starting from the initial guesses ψ_0 and ψ_1 computed in Sect. 15.4, the secant method converges to the unique value of $\psi > 0$ solving Eq. (15.8). In our experiments, due to the accuracy of the initial guesses, the iterations converge to a tolerance of 10^{-12} within 5 iterations. Once ψ has been obtained, χ can be determined from Eq. (15.9). Then, (α, β) are computed from (χ, ψ) using Eq. (15.6), which in turn yields (F_x, F_z) from Eq. (15.4). The cable profile can be easily determined from parametric closed-form Irvine expressions available in literature [3] in terms of (F_x, F_z) . The entire workflow is presented in Algorithm 1.

A test data set of 10,000 random samples is generated in the range $x \in [0.01, 10]$, $z \in [-10, -0.1]$, and $L \in [0.01, 50]$ along with k > 0.95. The cable properties chosen are as follows:

$$\mu = 0.079 \text{ kg m}^{-1}, \quad A = 4\pi \cdot 10^{-6} \text{ m}^2, \quad E = 100 \text{ GPa},$$

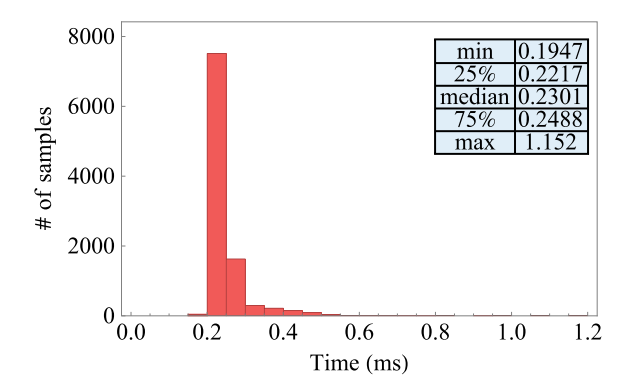
and acceleration due to gravity $g = 9.81 \text{ m s}^{-2}$. Using this dataset, we demonstrate that (F_x, F_z) can be computed in approximately 0.25 milliseconds on average using Algorithm 1, with computations executed in Wolfram Mathematica [8] on an Intel[®] CoreTM 2.80 GHz system. Figure 15.3 presents a histogram of the computation times

Algorithm 1 Solving for Cable Tension in Irvine Sagging Cable

```
Initialize system parameters: x > 0, z \in \mathbb{R}, L > 0, \mu > 0, g \leftarrow 9.81, E > 0, A > 0
Set algorithm constants: a \leftarrow 2.120, b \leftarrow 0.413, tol \leftarrow 10^{-12}, j_{\text{max}} \leftarrow 25
Calculate normalized parameters: x_m \leftarrow \frac{x}{L}, z_m \leftarrow \frac{z}{L}
Calculate \varepsilon \leftarrow \frac{\mu g L}{2EA}, k \leftarrow \frac{\sqrt{1-z_m^2}}{x_m}
Define the non-algebraic function f(\psi) := \left(\frac{x_m \sinh[\psi]}{\varepsilon + \psi}\right)^2 + \left(\frac{z_m}{\varepsilon \coth[\psi] + 1}\right)^2 - 1
     \psi_0 \leftarrow \sinh^{-1} \left[ k \sinh^{-1} \left[ k \sinh^{-1} \left[ k a(k-1)^b \right] \right] \right]
\psi_1 \leftarrow \psi_0 \left( 1 + \frac{k\psi_0 - \sinh[\psi_0]}{\cosh[\psi_0]\psi_0 - \sinh[\psi_0]} \right)
else
      \psi_0 \leftarrow 0 \\ \psi_1 \leftarrow \frac{\varepsilon}{\sqrt{x_m^2 + z_m^2}}
Compute the function residues F_0 \leftarrow f(\psi_0) and F_1 \leftarrow f(\psi_1)
i \leftarrow 0
while j < j_{max} do
      Compute the next approximation of \psi using the secant method: \psi_{\text{next}} \leftarrow \psi_1 - F_1 \cdot \frac{\psi_1 - \psi_0}{F_1 - F_0}
      if |\psi_{\text{next}} - \psi_1| < \text{tol then}
            Converged: \psi_{\text{next}} is the solution for \psi
            break
      end if
       \psi_0 \leftarrow \psi_1, F_0 \leftarrow F_1
       \psi_1 \leftarrow \psi_{\text{next}}, F_1 \leftarrow f(\psi_{\text{next}})
      j \leftarrow j + 1
end while
if j = j_{\text{max}} then
      Not converged within j_{max} iterations
      return error
\chi \leftarrow \tanh^{-1} \left[ \frac{z_m}{\varepsilon \coth[\psi] + 1} \right]
\alpha \leftarrow \chi + \psi, \beta \leftarrow \chi - \psi
F_x \leftarrow \frac{\mu g L}{\sinh[\alpha] - \sinh[\beta]}, F_z \leftarrow \frac{\mu g L \sinh[\alpha]}{\sinh[\alpha] - \sinh[\beta]}
return F_x, F_z
```

for solving each sample in the test dataset. The same algorithm, employing Newton's method instead of the secant method, takes about 0.3 milliseconds on average. This justifies the choice of the secant method in this case, emphasizing the accuracy of the proposed guess function.

Fig. 15.3 Histogram of computation time for a random test data set of 10,000 samples



15.6 Summary

This work introduced a new algorithm for determining tension forces in sagging cables for any given valid set of geometric and material parameters. We prove that this non-algebraic system admits a unique solution and show that it can be found in real-time using the secant method with carefully chosen initial guesses. Notably, this work offers valuable insights for modeling CDPRs. When developing neural network models for the kineto-statics of large CDPRs, e.g., [2, 5], it may be sufficient, subject to further investigation, to develop a kinematic model instead of a kineto-static model because forces and cable profiles can be back-calculated uniquely in real-time.

References

- Baskar, A., Plecnik, M., Hauenstein, J.D., Wampler, C.W.: A numerical continuation approach using monodromy to solve the forward kinematics of cable-driven parallel robots with sagging cables. Mech. Mach. Theory 195, 105609 (2024)
- Chawla, I., Pathak, P., Notash, L., Samantaray, A., Li, Q., Sharma, U.: Inverse and forward kineto-static solution of a large-scale cable-driven parallel robot using neural networks. Mech. Mach. Theory 179, 105107 (2023)
- 3. Irvine, H.M.: Cable Structures. The MIT Press Series in Structural Mechanics (1981)
- Khovanskii, A.: Fewnomials and Pfaff manifolds. In: Proceedings of the International Congress of Mathematicians, vol. 1, p. 2 (1983)
- Merlet, J.P.: Advances in the use of neural network for solving the direct kinematics of CDPR with sagging cables. In: International Conference on Cable-Driven Parallel Robots, pp. 30–39. Springer (2023)
- Merlet, J.-P.: Irvine cable equations and neural networks. In: Okada, M. (ed.) Advances in Mechanism and Machine Science, pp. 356–366. Springer Nature Switzerland, Cham (2023)
- 7. Sharma, A.K., Sinha, S.S., Kumar, R., Saha, S.K.: Semi-analytical solution for static and quasistatic analysis of an inextensible cable. Int. J. Solids Struct. **234**, 111296 (2022)
- 8. Wolfram Research Inc.: Mathematica, Version 13.2.0.0, Champaign, IL, 2023